REGULAR PAPER

Energy Efficiency of theVulcanization Process of a Bicycle Tyre

Lohit Kumar Pentakota[1] · Paolo Albertelli[2] · Matteo Strano[2]

Abstract

The production of tyres is one of the most energy consuming manufacturing activities in the rubber sector. In the production cycle of a tyre, the curing operation has the maximum energy loss. This is mostly due to the extensive use of steam as a source of heat and pressure in the vulcanization process. To the author's knowledge, no scientific work is available in the literature where the energy efficiency of a tyre vulcanization press is estimated by means of a comprehensive model of all main components, including the moulds, the press with its heated plates, the bladder and, of course, the tyre. The present work aims at filling this gap. First, the press used for developing the model is described, along with its components and its typical product, a bicycle tyre. The instruments used for measuring flow rates, temperatures and pressures are also listed. Then, a numerical model is presented, that predicts the energy transfers occurring in the vulcanization press during a full process cycle. The numerical model, developed with the software Simcenter Amesim 2021.1, has been validated by means of measurements taken at the press. The results indicate that the amount of energy which is actually consumed by the tyre for its reticulation process amounts to less than 1% of the total energy expenditure. The paper demonstrates that the tyre industry is in urgent need of an electrification conversion of the traditional steam-based processes.

Keywords Rubber curing · Mould heating · Energy efficiency · Simulation

1 Introduction

About 1.5 billion tyres are produced every year around the world [1], ranging from small and lightweight bicycle tyres to huge and heavy airplane tyres, and their environmental impact is of paramount importance. During their service life, tyre are a source of polluting microplastics [2]; at the end of their service, wasted tyres are a major source of energy consumption and pollution [3]. Furthermore, the tyre industrial production sector is one of the most energy consuming manufacturing activities in the rubber sector [4]. Out of the annual production of rubber around 50% of material usage is for tyre industries [5]. The manufacturing of tyres

around the world almost have standardized processes and machinery. The process can be divided into four main steps: manufacturing and processing of raw materials and subcomponents, green tyre building, tyre curing or vulcanization, final inspections of the product. Energy is needed for all the steps in the production cycle and it represents one of the largest costs in this industry [6], not only because of the direct energy expenditures, but also because of the carbon taxes and right costs [7].

In the entire tyre manufacturing process, the curing cycle has the maximum energy loss [8, 9]. This is mostly due to the extensive use of steam as a source of heat and pressure in the vulcanization process [10]. The inconvenience of using steam is acknowledged in the literature [11], but very few works directly address the quantification of energy losses. Direct greenhouse gas emissions from the plants are due to natural gas used in heat and steam production, while electricity consumption causes indirect greenhouse gas emissions [12]. Decarbonising energy demanding industries through electrification is a common and recent trend [13], and the tyre industry would also greatly benefit from conversion of heating based on steam to heating based on electrified processes. There are many reasons why in the

✉ Matteo Strano
matteo.strano@polimi.it

Lohit Kumar Pentakota
lohitkumar.pentakota@mail.polimi.it

Paolo Albertelli
paolo.albertelli@polimi.it

1 STIIMA-CNR, Via Alfonso Corti 12, 20133 Milan, Italy

2 Dipartimento Di Meccanica, Politecnico Di Milano, Via La Masa 1, 20156 Milan, Italy

🖉 Springer KSPE

vulcanization process energy is lost [14]: the presence of poorly insulated piping and complex installations, excessive discharging capacity of some steam traps, poor insulation of the flange valves, pressure reducers and covers of the curing cans, steam leaking, etc. Improving the energy efficiency of the vulcanization process would represent a significant improvement of the entire rubber manufacturing industry. The energetic efficiency could be improved by means of several remedies and actions, e.g. by reducing the outgoing radiation, preheating the curing moulds, shortening the time for exchanging dies and parts in the press, changing the heating system into more efficient techniques.

A more efficient way of heating the moulds, instead of steam, would be by electric induction heating [15]. Zhang and co-authors [16] developed a kind of curing technology of direct pressure shaping with inner mould and a controlled telescopic metal mould with high heat conductivity and electromagnetic induction heating. In other fields of the polymer industry, even more advanced techniques for conformal heating of moulds are being experimented [17], and they might very well be transferred to the tire curing sector. However, before any improvement can be done, it is essential to develop a deep knowledge, i.e., to model, how the energy flows inside the vulcanization process and to be able to estimate the efficiency of all steps and tools of the process. Although other modern and efficient heating techniques could be used for curing, such microwave heating [18] or infrared heating [19], no practical application of these potential technologies is known in the field.

Many models have been published regarding vulcanization process during the years. However, the vast majority of them are focused on the thermal and kinetic behaviour of rubber during its curing from a theoretical and empirical point of view, with the aim of predicting the thermal field history inside the tyre, such as the works by Yan and Tong [20] or by Han et al. [21] and many others. When the heat transfer is modelled, as in [22], this is done to predict the degree of cure or to avoid overcuring, but not to predict the energetic efficiency of the equipment. These models represent a solid base for optimization of the process with respect to product quality [23], but they are not aimed at fulfilling energy efficiency requirements nor they consider the vulcanization press as a system.

Only a limited number of scientific works directly address the problem of estimating energy losses and efficiency of a tyre curing plants. As an example, an economic analysis based on energy costs in a real case study is made in [5] for a whole plant in Sweden. Another study proposed a statistical model capable of predicting energy efficiency from simple operational variables such as vulcanization temperature, pressure and time as well as from ambient conditions [24]. The model relates these influencing factors to the theoretical energy consumption (TE) of the process, using mathematical equations to represent all the process sub-steps where energy is employed. This theoretical value is confronted to the real one measured from the industrial equipment consumptions, called direct energy (DE), obtaining an efficiency value of the whole vulcanization process.

The EFR_{equip} is defined by the ratio of the theoretical energy consumption (TE) over the direct energy (DE), and it can be used as an energy efficiency indicator [25]:

$$EFR_{equip} = \frac{TE}{DE} \tag{1}$$

with $0 < EFR_{equip} < 1$.

The above definition of energy efficiency can be used for different purposes, depending on how TE is determined or defined. As an example, Eq. (1) can be used to monitor and evaluate the health of the equipment and its thermal insulating conditions over time. In this case TE should approach 1 for a well-maintained equipment and it must include the vulcanization energy plus all the energy components required to heat the moulds, all the theoretical losses to the environment and any other predictable energy requirement for a given plant. Following the same line of studies, in [26] a method was developed to detect heat loss due to fault on the steam traps or insulating whenever they appear in a tyre vulcanizing workshop. In the present paper, TE is defined as the difference between the total external energy which is spent during one curing cycle and (DE) and the energy which is lost in some form.

Most works in the literature estimate the energy efficiency at the factory or shop floor level. To the author's knowledge, no scientific work is available where the energy efficiency of a tyre vulcanization press is estimated at the machine level. Schmidt and co-authors have presented simple models for customized prediction of energy consumption for 9 different types of manufacturing machines, but they did not include any rubber curing or forming press in their study [27]. The present work aims at filling this gap. To this purpose, a comprehensive model of all main components, including the moulds, the press with its heated plates, the bladder and, of course, the tyre, including all the process phases (warm up and curing) has been developed. The proposed model is built around a specific case study: the vulcanization of a bicycle tyre. While the vulcanization process is exothermic, the tyre still requires some external energy to start the curing process (it is called induction energy) and to keep the temperature high during the curing, i.e. to sustain the curing process [28]. The sum of these two energy quantities, required by the tyre mass, will be called vulcanization energy (VE) as follows. Obviously, VE is much smaller than TE or DE,

because a much larger energy than VE is required to keep the moulds warm, to move the press slide, to inflate the bladder, etc. In other words, while DE includes all the energy requirements to operate the machinery, VE only includes the heat received by the tyre. The paper aims at estimating the overall efficiency of the vulcanization process, measured as:

$$EFR_{vulca} = \frac{VE}{DE} \qquad (2)$$

where VE is the vulcanization energy absorbed by the tyre during a vulcanization cycle. Since VE < < DE, very small efficiency values $EFR_{vulca} << EFR_{equip}$ are expected.

Although in the rubber industry there is a general belief that the energy efficiency of the vulcanization process is very low, no number is available in the scientific literature to quantify EFR_{vulca} or some similar indicator. The only available study is focused onto the injection moulding of elastomers [29]. This study shows that only 8% of the total energy is used for the vulcanization of the rubber, the rest is lost by conduction and convection, because of the need of heating the moulds. A preliminary study run on vulcanization of bicycle tyres [30], based on a purely analytical model of heat exchange phenomena in the tooling, has calculated an even lower value: 5%. In this paper, a simulation model is presented, validated by experimental measurements at a vulcanization press, which allows to precisely estimate the value of EFR_{vulca} for a specific process.
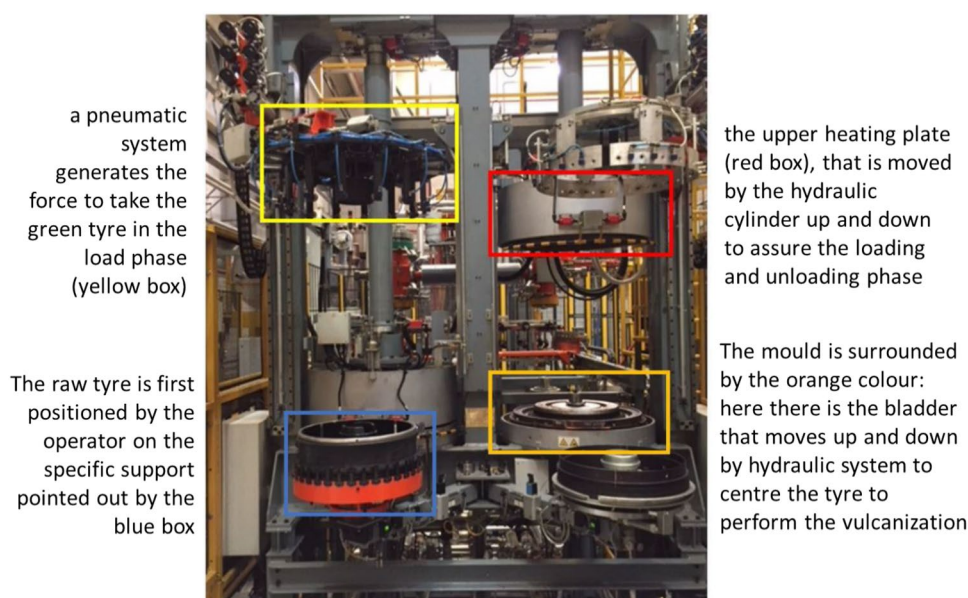
2 Vulcanization equipment and process

2.1 The equipment

A vulcanization equipment is made of six main parts: a universal (hydraulic) press, two hot plates, the moulds, a bladder, a central group and a clamping structure. A schematic figure on their relative position when the press is closed can be seen in Fig. 1. The main structure supporting all the specific and auxiliary equipment for tyre curing operation is formed by a hydraulic press with two pistons. This allows to have two vulcanization chambers. Hot plates and bladder are the only sources of heating of the whole system, which, in the present case, is provided by steam. This heating medium flows inside inner channels embedded in the hot plates, which in turn heat the dies by conduction. A bladder is placed inside the tyre and is also filled with steam, at higher pressure and temperature than in the hot plates. As the tyre must be introduced and released at the beginning and end of vulcanization cycle respectively, some of the parts are movable. In other words, the central group, the bladder and the press have a dynamic action allowing to open and close the curing tooling (or chamber), shown in Fig. 1.

The press and its controls enable the independent movement of each chamber, which can be opened and closed not simultaneously. However, the temperature regulation is in common for both chambers because some of the auxiliary equipment and steam feeding piping are unique and belong to a centralized plant system.

In the energetic model here proposed, energy consumption and efficiency have been studied only for one of the chambers, independently from the other.

Fig. 1 Hydraulic press for vulcanization of a bicycle tyre

a pneumatic system generates the force to take the green tyre in the load phase (yellow box)

The raw tyre is first positioned by the operator on the specific support pointed out by the blue box

the upper heating plate (red box), that is moved by the hydraulic cylinder up and down to assure the loading and unloading phase

The mould is surrounded by the orange colour: here there is the bladder that moves up and down by hydraulic system to centre the tyre to perform the vulcanization
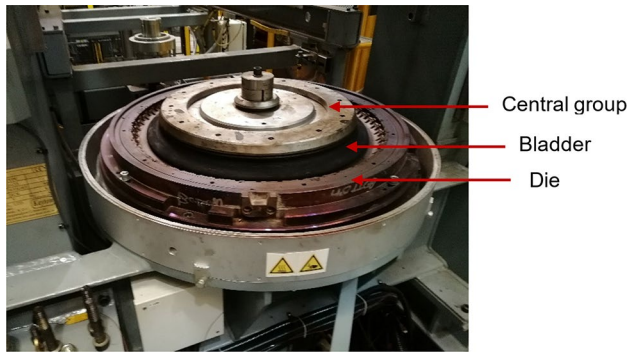
Fig. 2 Open vulcanization press. Detail on central group, bladder and bottom die

Moulds (or dies) are the passive part, responsible for the moulding of the green tyre. The pressure provided by the bladder (active part) compresses the tyre against the dies so that the characteristic external geometry of the tyre, which confers some of the most important performance attributes such as rolling resistance or grip, are achieved during this phase due to the dies imprinted surface geometry. In Fig. 2 a generic complete tooling set for a car tyre is shown, while in the next Fig. 3 the tooling set used in the present study is shown.
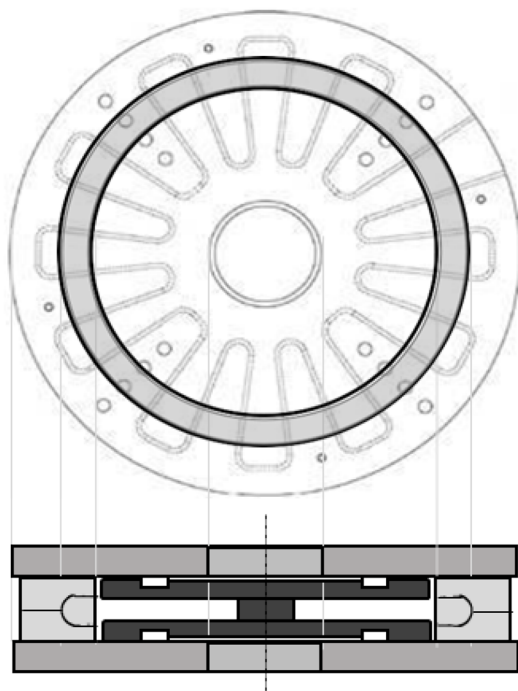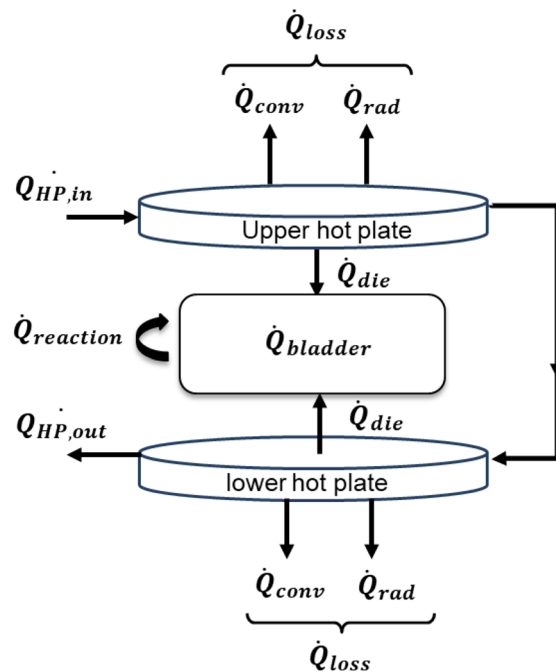
An upper and a lower hot plate provide heat to the process. In a two-halves tooling set, used for small tyres, like the one modelled in this work, the hot plates are the only external source of heating. The heat plates are circular, made of steel. Hot plates are heated by steam flowing through an inner channel with circular cross-section of 15 mm diameter. An approximate layout of the inner channel is shown in Fig. 3. The figure also shows the proposed modelling for the heat fluxes and losses in the tooling.

Steam at the inlet section is, ideally, saturated steam that will tend to condensate when the hot plate is transferring heat to the tyre for curing it. So, at the outlet section, a mix of steam and liquid water is expected to exit, generally.

The bladder is a deformable inflatable body generally made of a thermally conductive butyl rubber of 4- or 5-mm thickness. It is filled with high pressure steam or other heating medium to transfer thermal energy to the green tyre as well as to provide the mechanical action needed to make the rubber flows inside the dies imprinted pattern. Bladder surface is designed to prevent air trapping and bubbles formation between the bladder and the tyre, which would cause superficial defects. The bladder shape is like a toroid whose internal radius is fixed to the central group. The vertical movement of the central group, together with the steam filling, controls the bladder deformation, facilitating its adjustment to the dies when press is closing. The central group

Fig. 3 Qualitative detail of hot plate inner channel, showing also the tyre position (top); hot table and dies section side view (bottom). In the right part of the figure the heat input and output flows are shown: the convective and radiativo losses from the upper and lower moulds and plates, the input entalpy of the steam entering the upper plate, the energy lost with the steam that flows out of the lower plate, the heat enetring the system through the inflated bladder

is formed by two cylindrical plates and a central hydraulic piston. It facilitates the closing dies operation by lowering its upper plate, to deform the bladder to an adequate geometry to fit inside the dies. It also has a similar function during the die opening phase, when it facilitates the detaching of the bladder from the inner surface of the dies.

2.2 Measurement instruments

During the curing process, different types of sensors are used for measuring mass flow rates, pressures and temperatures in the press equipment. A schematic representation of the localization of the sensors is reported in Fig. 4. The details of the sensors installed at the inlet of the hot plates, at the outlet of the hot plates, at the outlet of the condenser and at the inlet and outlet of the bladder are reported in Table 1.

Flowmeters based on Coriolis technology were installed in all the positions, except at the hot plates inlet since it was supposed that in that plant position the flow is entirely made of steam, being closer to the steam generator. Indeed, the Coriolis based flowmeters are more suitable that Vortex based flowmeters for measuring biphasic flows.

The sensor signals were acquired using National Instruments equipment, setting a sample rate of 5 Hz. Specifically, a compact DAQ Ni cDAQ-9139 and three acquisition boards were used, respectively the NI9205, the NI9209 and the NI9923.

2.3 The process

Tyre vulcanization refers to the curing reaction necessary for a green tyre to become a product with the required
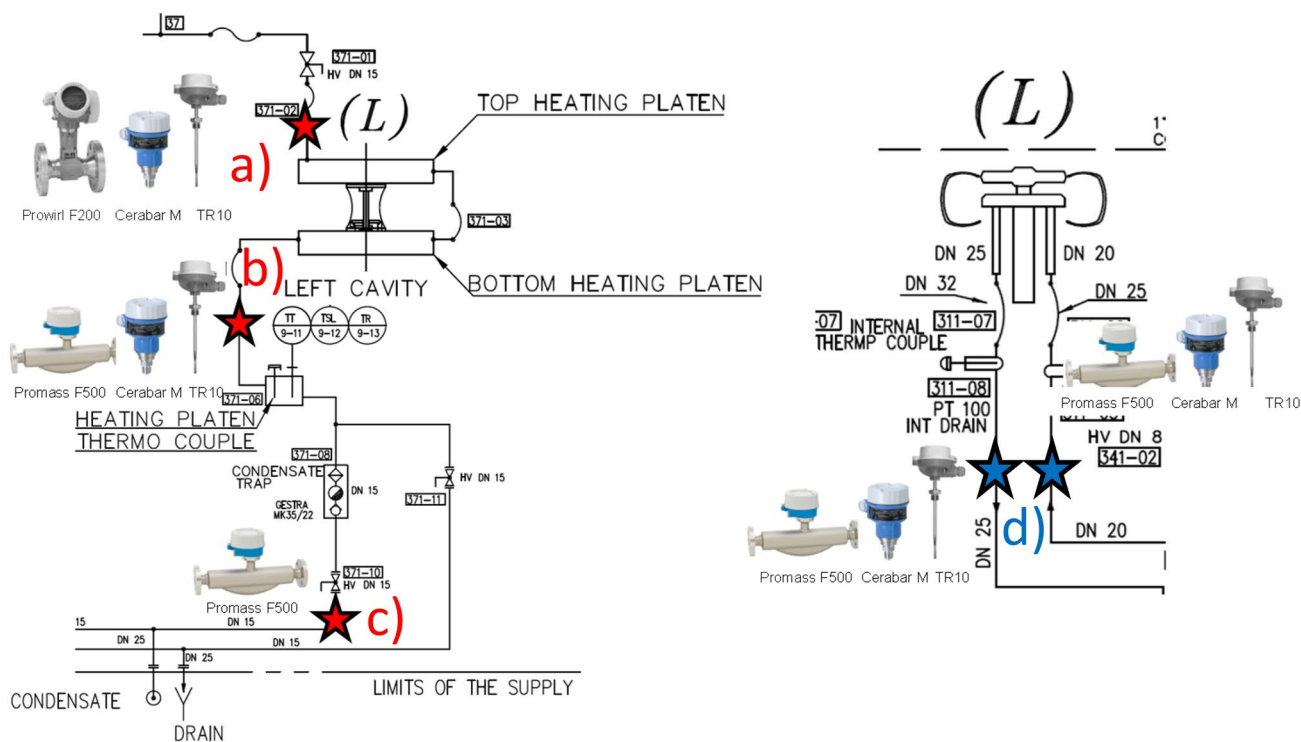

Fig. 4 Layout of sensors; **a** hot-plates inlet, **b** outer hot plates, **c** outer condenser and **d** inlet and outlet of the bladder

Table 1 List, purpose and location of sensor in the tooling setup

Measured quantity	Sensor	Location of sensor (Figs. 4 and 5)
Flow rate	Endress Hauser Promass F 500, 8F5B08 (Coriolis technology)	Outlet of bottom plate, Inlet of bladder, Outlet of bladder, outlet of (after the) condenser
Flow rate	Endress Hauser- Prowirl F 200, 77F2B15 (Vortex technology)	Inlet of top plate
Pressure	Endress Hauser—Cerabar M PMP51	Inlet of top plate, Outlet of bottom plate, Inlet of bladder, Outlet of bladder
Temperature	Endress Hauser—TR10	Inlet of top plate, Outlet of bottom plate, Inlet of bladder, Outlet of bladder

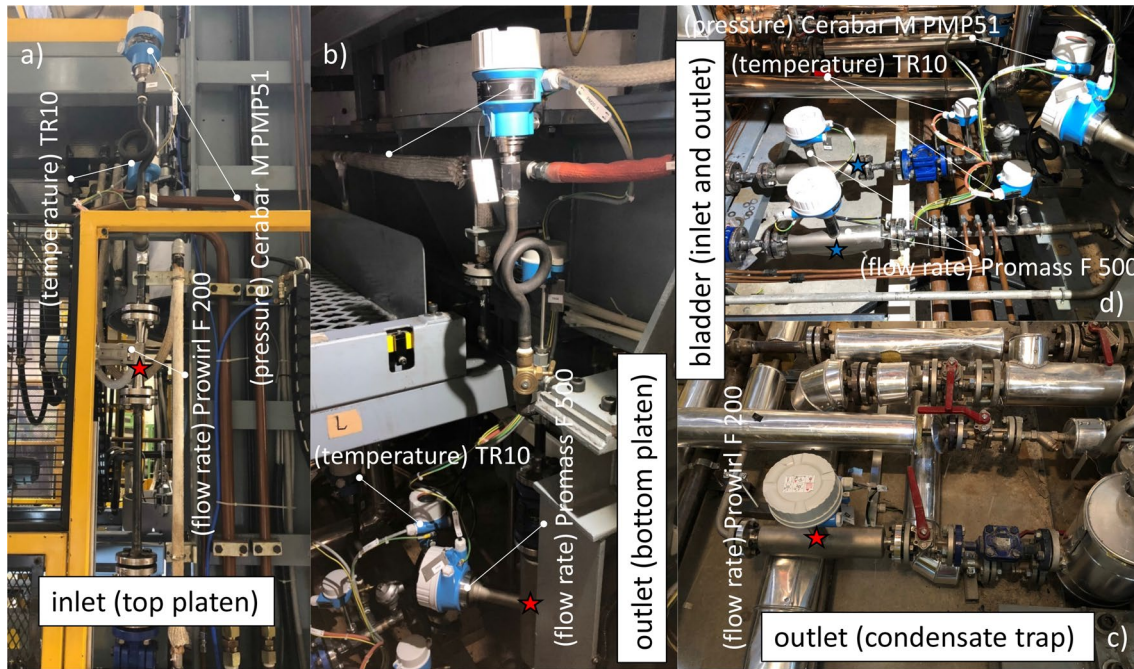**Fig. 5** Images of sensors; **a** hot-plates inlet, **b** outer hot plates, **c** outer condenser and **d** inlet and outlet of the bladder
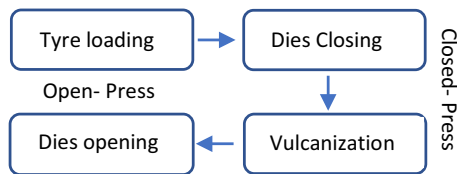

Fig. 6 One cycle sequence of the vulcanization press

mechanical properties for its use. Several papers and thermo-mechanical models of the process are available in the scientific literature that describe and model the kinetics of the transformation process [31]. Vulcanization tends to increase elasticity and reduce plasticity, facilitating the return of the rubbery material to its original shape. This improvement in the mechanical properties responds to the formation of a crosslinked molecular network. To trigger and accelerate the reaction, rubber must be heated. Also, reaction accelerators and activators must be used to reduce the overall time needed. Non-accelerated vulcanization accomplished by elemental sulphur can require 5 h at 140 °C while, by the addition of small quantities of beforementioned agents, time can be shortened to a few minutes [32]. The vulcanization reaction is exothermic [33], and the heat reaction might have an impact on curing quality. However, in this research, this phenomenon has not been taken into consideration, because its energetic contribution is negligible. It is well known that the exothermic enthalpy ranges between 5 and 40 kJ/kg [34], i.e. it amounts to a maximum of about 10 kJ for a 250 g tyre,

while the DE energy spent in the process is several orders of magnitude larger.

A complete cycle of the vulcanization press includes 5 main steps: green tyre charging, dies closing, vulcanization, dies opening and tyre discharge; illustrated in Fig. 6. The main step is the vulcanization when green tyre is cured.

As Fig. 1 shows, there are two main process stages: open die (or open press) and closed die (or closed press).

2.3.1 Open press

When the curing cycle is over and the press must revert to the open state, an outlet valve is opened to allow the discharge of steam and formed condense, reducing the inner pressure inside the bladder. Once the top set of tools has been risen, the vulcanized tyre is still in contact with the bladder, which, due to the elevated temperature and pressure, is usually partly attached to the product. Finally, an unloading auxiliary support is placed under the tyre to collect it. That part of the bladder that remains in contact to the tyre is detached from it. For enhancing this process, a vacuum line is available and connected to the bladder, facilitating the tyre removal.

2.3.2 Closed press

When the tyre and bladder are in contact, dies closing can begin by lowering the top moving part of the press. In other words, the set of hot plate, dies and clamping fixture. A

Table 2 Basic variables of the vulcanization tooling and process of a racing bike tyre

Variable	Value	Units
Tyre mass	0.205	kg
Vulcanization time	5.723	min
Bladder inner steam pressure	12.5	bar
Bladder inner steam temperature	197.5	°C
Die inner steam pressure	10.11	bar
Die inner steam temperature	189.5	°C
Hot plate diameter	0.915	m
Hot plate height	0.052	m
Hot plate volume	0.0342	m^3
Die diameter	0.873	m
Die height	0.075	m
Die volume	0.0449	m
Total volume of upper press or lower press (hot plate and die together)	0.0791	m^3
Hot plate surface and Die surface area	(0.6576 + 0.5986)	m^2

Fig. 7 Side and tread views of the tyre used in the investigated process

small bicycle tyre can be produced with only about 10 to 15 bar of relative pressure, due to its low thickness and low surface complexity. Even though condensation inside the bladder is inevitable, it is not beneficial. Moreover, it produces water droplets that coalesce forming hot zones, detrimental for product quality as they can lead to overcuring in certain spots, so it should be reduced when possible. The saturation temperature of steam at the operating conditions is around 200 °C inside the bladder, which is designed to get a final tyre temperature of 180 °C. For the vulcanization of a bike tyre, the curing time is about 5 min. In conclusion, three main parameters govern the process: temperature, pressure and time. Among them, temperature and time are the most important as they provide the total heat transferred to the tyre, which is critical for the final product characteristics and quality. Pressure seems to have a secondary role, even though it is related to temperature in the case of steam heating as beforementioned. In Table 2, the main variables and parameters of the vulcanization process are shown for the

investigated example, a road racing bike tyre of 670 mm outer diameter, 70 mm width, thickness ranging from 2 to 3 mm and 205 g weight (Fig. 7).

The process variables of the curing phase have been measured for about 2200 s, a time span that covers almost 5 curing cycles. In Fig. 8 the plots of the some of the measured variables are shown. The steam that flows inside the hot plates amounts to a mass flow rate of a little more than 6 kg/h. The maximum pressure at the bladder is above 12 bar. The temperature at the bladder oscillates between about 120 and 190 °C.

3 A numerical simulation model

A simulation model has been developed with the software *Simcenter Amesim 2019,* able to predict the mass flow rate of steam used for heating the moulds, the pressures and the state of the fluid (liquid or steam) at the outlet of the bottom please and at the outlet of the bladder. This software tool allows the use of ready-to-use multi-physics libraries, including libraries for thermal management and fluid system simulation [35]. The software implements a lumped parameter transient numerical model which can simulate the transient operation of a heat pipe where a fluid flows. It has been frequently used in the scientific literature for solving thermal problems for single-phase [36] or two-phase flows [37]. Both solid components (i.e., the hot plates and the moulds) and fluidic domains (i.e., the two-phase steam/water flow) are subdivided into a limited number of control volumes, called "lumps", each characterized by a thermodynamic status. Lumps are connected to each other by means of resistive, capacitive and inductive elements, modelling different physical phenomena (i.e., thermal or flow resistance, thermal inertia or fluid inertia). Each lump is governed by an ordinary differential equation so that the overall transient problem can be reduced to a linear system, numerically solved. Three main libraries have been used:

- Two-phase library. some elements of the two-phase library have been used to monitor phase change occurrences, energy and mass transport. They allow computation of pressure losses, temperature levels, mass flow rates and enthalpy flow rates, steam mass fraction. Each lump may model internal convective heat transfer (single phase or convective boiling or condensation), and external flow convective heat transfer (moist air). Gravity in pipes is not accounted for and the model is 1D with homogenous flow (no slip between the phases, homogenous temperature in the volume). The two-phase fluid obeys the Helmholtz energy law (as in [38]) for water mixtures. The Maxwell criterion is used to calculate the fluid saturation curve (as in [39]).
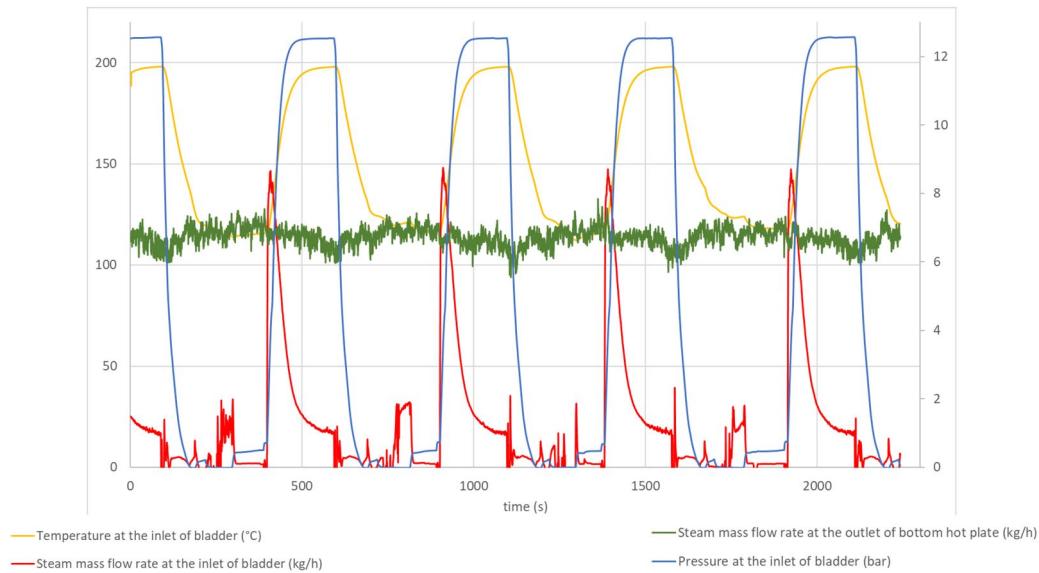
Fig. 8 Measured variables during some consecutive curing cycles; temperature (yellow line) and inlet mass flow rate (red line) at the bladder are reported on the left vertical axis; the steam mass flow rate at the outlet of bottom plate (green line) and the pressure at bladder (blue line) are reported on the right vertical axis

- Thermal library. Elements of the thermal library have been used for the simulation of the solid parts of the system (i.e., the metal of the hot plates and the moulds, the rubber of the bladder and the tyre) and model their heat exchange to the environment and to the fluid flow. The thermal library is used to model transient heat transfer modes (conduction, free and forced convection, as well as radiation) between solid materials. It includes coupling elements (thermal ports) to the two-phase library, permitting the thermal interactions between solids and two-phase fluids (as in [40]). Few assumptions are made in each thermal lump: heat flow is 1d, solids are isotropic, temperature in the thermal capacities is homogenous.
- Mechanical library. Some elements of the mechanical library have been used to model the elasticity of the bladder which inflates under the pressure of the steam (as in [41] or in [42]).

The developed model allows to estimate the energy consumption and efficiency of the described press operations. The model can be described separately for the two phases of each chamber: open and closed press, as described in Sect. 2. The curing cycle of a racing bike tyre has been modelled, and the results have been compared to experimental measurements taken at the vulcanization press. Part of the experimental data has been used to determine some of the model boundary conditions (e.g., the steam temperature and pressure at the inlet of the heating piping) and part has been used to validate the model (e.g., mass flow rates).

3.1 Warm-up (open-press) phase

The warm-up phase is simulated assuming the tooling is still at room temperature, i.e. it is an operation that takes place only a very limited number of times, for a press that operates at full productivity. In fact, it is typical of tyre vulcanization plants to operate 24 h a day, 7 days a week. Warming up is required after a production change, or after maintenance or after some vacation break.

This phase can be described with reference to Fig. 9, where a logical and simplified representation of the model is presented, and each component of the model has been given a number in round brackets. Warming-up is entirely conducted in an open-press condition, therefore the model considers the heating fluid as an open-pipe flow through the hot plates, when the moulds are open and there is no tyre in place nor the bladder is modelled. In the first transient phase, for the first 100 s, water is drained out of the system to speed up the preheating phase, until the fluid state reaches the condition of saturated steam not only at the inlet, but also at the at the outlet. The state of the fluid at the inlet is imposed to the model as a boundary condition. At the sink (the outlet boundary condition), the pressure is assumed to be at an atmospheric level.

Figure 9 is divided in three logical blocks: a block on the left called "Inlet boundary conditions", which indeed sets the inlet boundary conditions and the material properties; a central block that models the hot plates and the mould; a block on the right which sets the boundary conditions at the outlet.
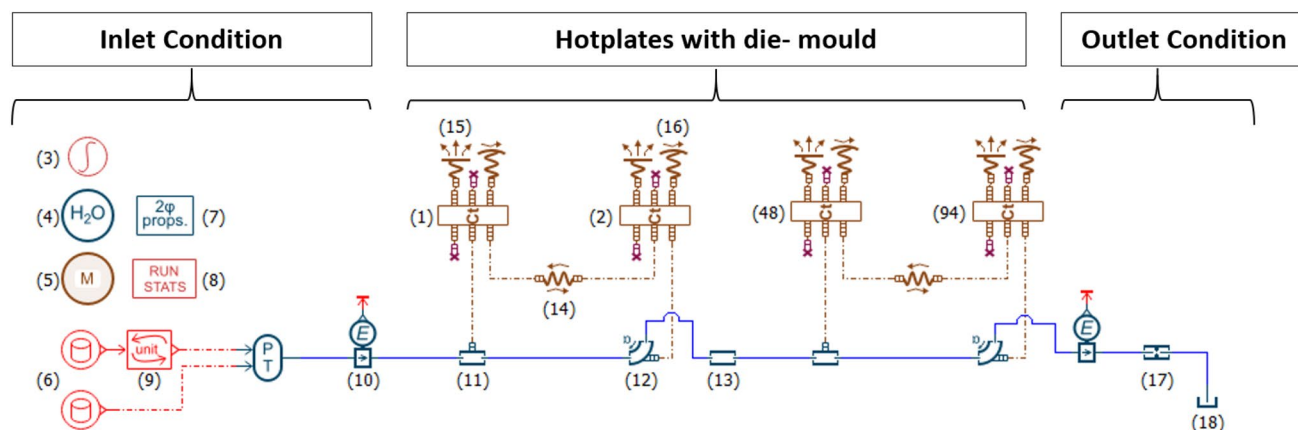
Fig. 9 Simplified logical representation of the Amesim simulation model of open press phase

3.1.1 Inlet boundary condition

A logical element called "sim parameters" (3) controls the simulation parameters, namely the error tolerance (set at 10^{-8}) in solving the equations and the maximum time step used in time resolution (set at 10^{-4} s). The "sim parameters" element is labelled with the number (3) in round brackets in Fig. 9. "H_2O" (4) determines the inlet state of the fluid, whereas the "2ϕ props" (7) models the 2-phases fluid properties. A parameter called "steam quality" represents the two-phases the fluid. It expresses the mass fraction of steam and assumes values between 0 (when the whole fluid is made of water) and 1 (when the pipe is entirely filled with steam). "M" (5) defines the material properties of both hot plates and mould. "Run Stats" (8) is the module that collects the numerical results of the simulation during post-processing. Based on the experimental measurements, the boundary condition at the inlet is set at specified pressure and temperature values, flowing through the hot plates for 2000s. The inlet boundary conditions in terms of pressure P and temperature T are given to the model as an input, using two dynamic timetables (6) for reading the experimental data as time-dependent signals. A "unit" converter (9) is used simply to convert the pressure from relative to absolute values.

3.1.2 Hot plates with die-mould

The central block of the system was built by modelling the piping as a sequence of straight (11) and bent (12) pipe lumps. The two-phase and the thermal libraries lumps are connected through thermal ports. The hot plates (upper and lower) are modelled as a sequence of 94 lumps which are dynamic thermal capacities: from (1), to (47) for the upper plate, and from (48) to (94) for the bottom plate. The 94 thermal lumps represent the combination of both hot plates and moulds, assumed to be made of the same material

characteristics (i.e., steel). Linear conductive heat transfer elements (14) are placed between the lumps. At each lump, heat losses are also considered of two types: convection losses and radiation losses to the environment. Convective (15) and radiative (16) components are therefore attached to the 94 lumps. An adiabatic pipe (13) is placed to connect the upper and lower hot plates.

3.1.3 Outlet condition

This block simply consists of a pipe with frictional pressure drops (17) and a sink tank (18) for closing the circuit, maintained at atmospheric conditions.

3.2 Curing (closed-press) phase

The model of the closed press phase, suitable for the curing phase, is logically represented in Fig. 10. As in Fig. 9, numbers in brackets are used to identify its logical blocks. After the preheating phase, the model is ready to vulcanize a tyre.

From a modelling point of view, the "inlet condition" and the "Hot plate with Mould" blocks will not change compared to the warm-up phase. As an addition to the previous model, the bladder and the tyre are now present, and a declaration of material properties (5) is required for them. The two kinds of rubber are considered to be very similar, hence the same material properties are given. The thermal material properties used are summarised in Table 3. Among the thermal properties, several recent studies in the literature have shown that the thermal expansion of rubber has an important role in the process, influencing the quality of the product. These studies are based on numerical models, namely finite element models [43]. However, while the expansion of the tyre does not directly influence the heat conduction phenomena. The epansion of the tyre might increase the coefficient of thermal
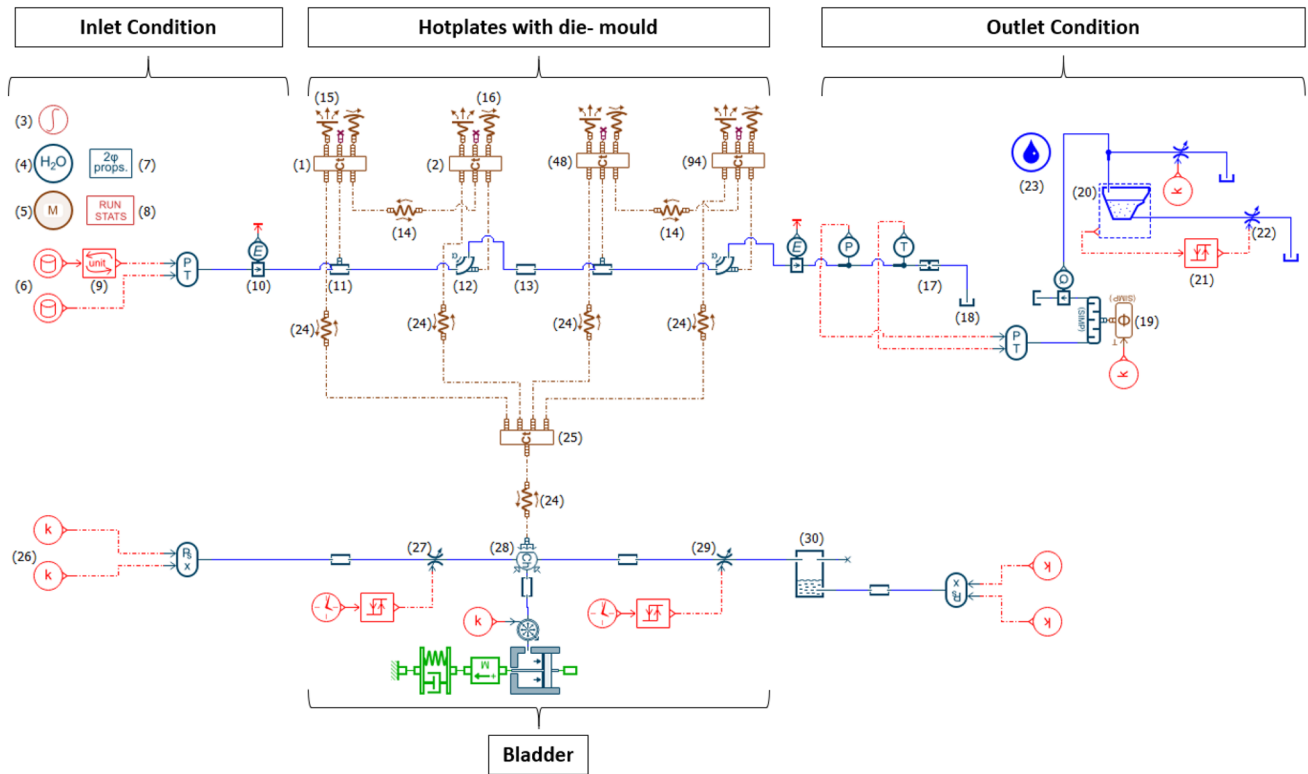
Fig. 10 Simplified logical representation of the Amesim Simulation model of curing phase

Table 3 Material properties of tyre, bladder and moulds

Material	Thermal Conductivity (W/m.k)	Density (kg/m³)	Specific heat (J/kg.k)
Both (Top & bottom plate + Die/mould): Steel	16.27	8230	502.48
Tyre & Bladder	0.15	1134	2010
Interfaces		Thermal Contact Conductance (W/m².k)	
Tyre/mould		83.33	

exchange (defined as the "thermal contact conductance" in the amesim model) at the interface between the rubber and the mould because of an increased pressure. However, pressure at the interface is dominated by the steam pressure in the bladder, and the additional contribution of thermal expansion is reasonably negligible.

3.2.1 Tyre

The tyre is modelled as a single mass lump (25) that exchange heat by conduction. Both the hot plates and bladder transfer heat to the tyre through conduction elements (24).

3.2.2 Bladder sub-model

Around the bladder (28) a whole sub-model is built, that runs simultaneously to the main model. The sub-model is fed with imposed inlet boundary conditions (26): a constant pressure of 13.88 bar and a parameter called "steam quality" that represents the input steam mass fraction. The steam enters the bladder through an inlet valve (27), following the experimentally measured profile. The fluid leaves the bladder through an outlet valve (29). Opening and closing conditions of both valves are controlled by two trigger elements. Downstream the outlet valve, a two-phase tank (30) has been placed which reduces the mean fluid velocity and allows for a positive mass flow rate. The thermal lump is coupled

with elements taken from the mechanical library, namely a series of a piston, a mass and a damper/spring, which are used to model the inflation of the bladder as the steam pressure increases.

3.2.3 Outlet condition

This block is modified with respect to the previous phase, in order to have a more complete description of the fluid condition over time at the outlet of bottom plate. In fact, in this phase, pressure and temperature are almost constant throughout the system, since they only decrease down respectively to 10 bar and 187–188 °C. Due to this reason, the fluid is entirely made of steam, but it is necessary to condense it after exiting, to discharge the flow to atmospheric conditions. Therefore, the outlet boundary condition was changed compared to the model of warm-up phase to implement a heat exchanger. A condenser model (i.e., a heat exchanger) (19) has been used to model what happens to the residual steam, after the fluid has transferred part of its enthalpy to the hot plates. Throughout the condenser, the volumetric flow rate is totally converted from steam to water, which eventually feeds the tank (20). The discharge valve (22) will be in open or closed according the maximum and minimum limits which have been set for the water level in the tank.

4 Results of the model and comparison to experimental values

4.1 Warm-up phase

Simulation of this phase has run for 2000s. All results clearly indicate the presence of an initial transient regime and a final steady state. The temporal profiles of pressure

and temperature at the outlet of bottom plate depend on two-phase flow frictional pressure drops which are calculated using the well-known McAdams correlation (homogeneous model) [44] and proper initialization conditions in the pipe elements. Two parameters have been fine-tuned to match the experimental results: the parameter of the frictional pressure drops at the outlet boundary condition and the heat transfer gain in the pipe elements (which influences the heat flow rate towards the hot plates).

The results are shown from Figs. 11, 12, 13. The experimental pressure profile at the outlet of the bottom plate is reproduced very well by the simulation, both in the transient and in the steady state (Fig. 11). The experimental temperature profile at the outlet of the bottom plate is generally well reproduced, although the model slightly overestimates the transient temperature and underestimates the steady state value (Fig. 12).

The mass flow rate is calculated mainly depending on the cross-sectional area and on pressure losses along the pipe elements. The measurements of mass flow rate at the inlet sensor are not very stable and reliable and, consequently, in the transient phase significant oscillations are evident; besides, a relevant difference can be observed between the inlet and outlet flows until 400 s. On the contrary, the steady state values, after 600 s, are well reproduced (Fig. 13).

Finally, the energy flows and the efficiency of the open press phase can be computed basing on the results of the model, as will be later shown in Sect. 5.

4.2 Curing phase

The experimental values have been monitored through 5 subsequent curing cycles. The model results have been compared to the experimental values of the 3rd, 4th and 5th cycles, with a consistent level of accuracy. The first and second cycles have not been used for validation, so to allow

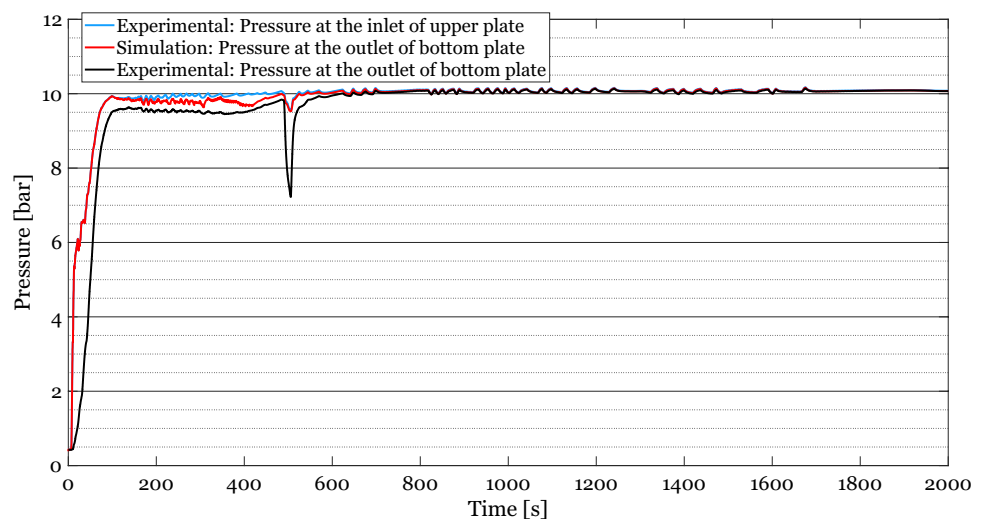**Fig. 11** Simulation vs. experimental pressure profiles at the inlet and outlet of hot plates

Fig. 12 Simulation vs. experimental temperature profiles at the inlet and outlet of hot plates
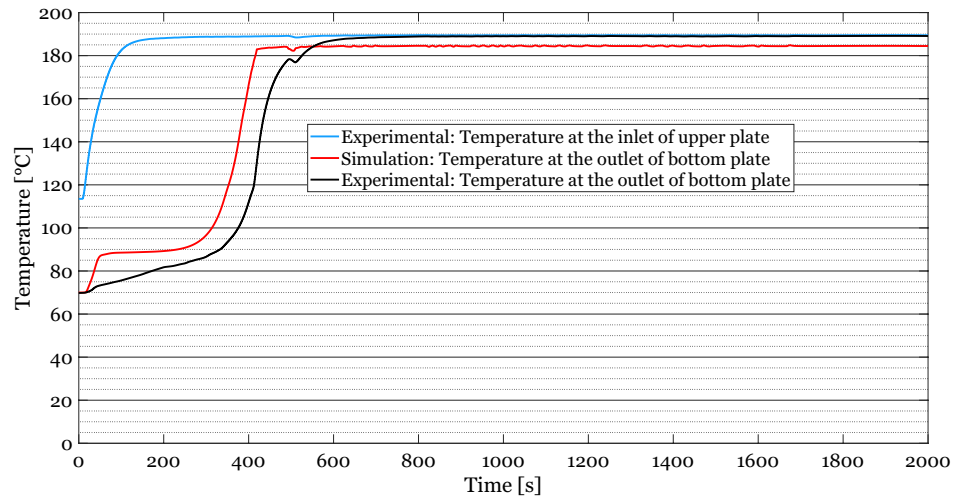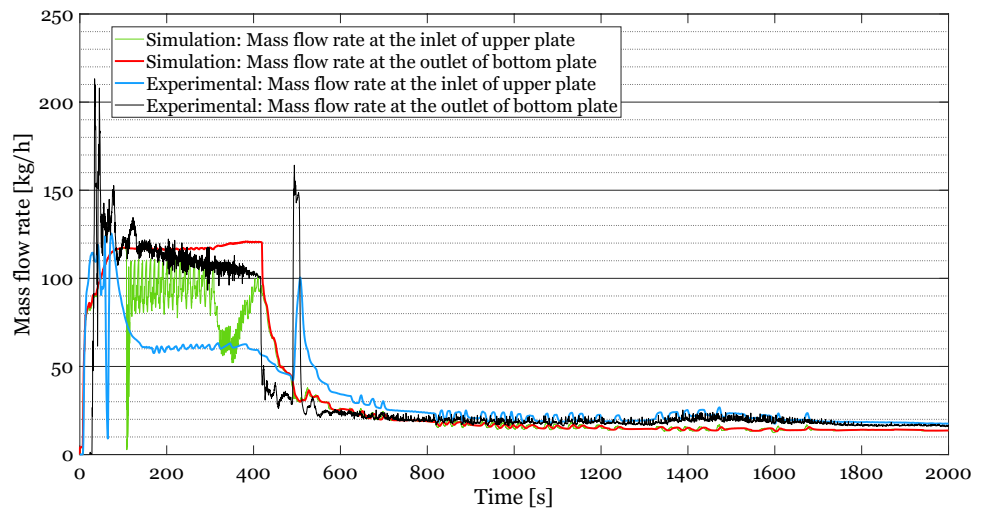

Fig. 13 Simulation vs. experimental fluid mass flow rates at the inlet and outlet of hot plates

the system to reach a regime condition. The simulation of each cycle has been run for about 340 s of simulated time. For brevity, in Fig. 8 the comparison of the third cycle is reported, starting from 900 s.

Sub-models have been added for simulating the bladder and the tyre. The initialization conditions of pipe elements and hot plates are different from the open press phase. The inlet flows are assumed at higher pressure (10.11 bar) and temperature (189 °C). For the bladder, the imposed boundary conditions are simply a constant pressure of 13.88 bar. As for the previous phase, a binary parameter called "steam quality" represents the saturated steam condition. The bladder diameter is 65 cm and its height is 6.5 cm, with a resulting inside volume of 21,500 cm³.

The cross section of the tyre is u-shaped, its inner diameter is 620 mm, the outer diameter is 670 mm, the thickness is between 2 and 3 mm, the width is 70 mm.

By analysing the experimental measurements, the process consumes about 3.5 kg of steam per cycle (0.6 kg for the steam pipes and 2.8 kg for the bladder) at an average pressure of 9 bar (including ramp-up); assuming a specific volume of 0.2 m³/kg, the consumed steam volume is a little more than 600,000 cm³ /cycle.

Measurements of fluid state after condensing has been carried out and the result is shown below ($X=0$); this condensed fluid will enter a discharge tank. A two-state behaviour over time of the mass flow rate at the outlet valve of the bottom plate has been observed in the model, with the simulated setup. This is due to the presence of a "condensate trap", shown in the left-bottom part of Fig. 4. It is a device that sometimes open, when there is enough condensate water, and lets it flow out. As a consequence, the flow rate oscillates between a high value when the trap is open and a low value when the trap is closed and this is confirmed by experimental evidence (Fig. 14). The real measured mass flow rate is affected by significant noise, and it is not "binary" as the model. However, the measured value oscillates between the same values (approximately 0.5 and

Fig. 14 Simulation vs. experimental mass flow rate at the outer valve and fluid states at both plates, outlet of condenser. The gas mass fraction is also shown
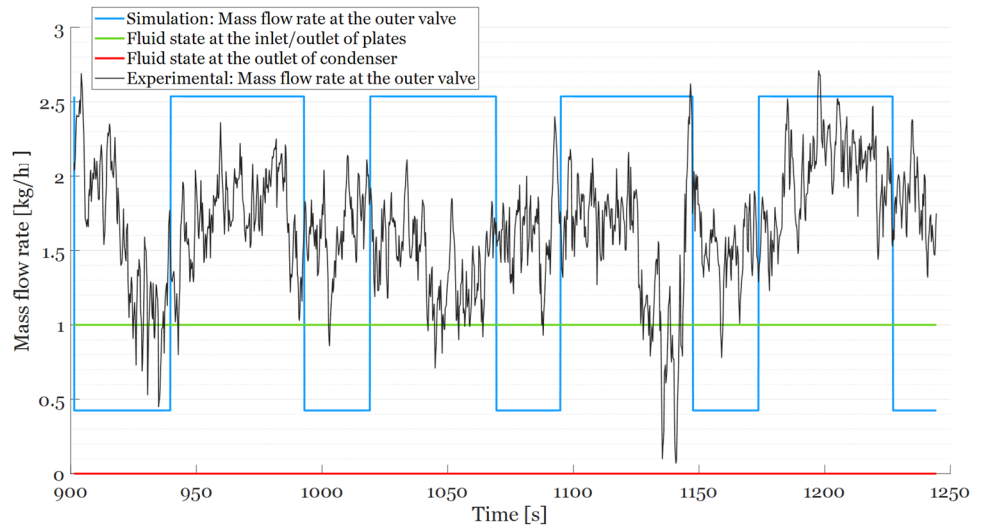

Table 4 Percentage differences between modeled and experimental values at the bottom hot plate

Time [s]	Outlet: pressure	Outlet: temperature	Outlet: mass flow rate	Inlet: mass flow rate
908	0.1%	0.09%	0.22%	−0.25%
950	0.11%	0.87%	0.43%	0.87%
1000	0.01%	1.00%	−0.63%	−0.64%
1050	0.11%	1.06%	−2.33%	−2.28%
1100	0.11%	1.15%	8.10%	−8.10%
1150	0.1%	1.21%	−4.82%	−4.81%
1200	0.11%	1.31%	−5.88%	−5.88%
1244.4	0.1%	1.45%	−1.60%	−1.59%

2.5) and the average mass flow rate over the time span is similar to the simulated value. The mean flow rate in that time span is 1.98 kg/h for the real curve and 1.72 kg/h for the simulated profile.

In order to further validate the model, Table 4 presents the average calculated percentage difference between the simulation vs. the experimental results at the bottom plate in terms of pressure, temperature, and mass flow rate.

4.3 Bladder sub-model

The experimental pressure profiles at the outlet of the inlet valve and at the outlet of the bladder are almost overlapped in the steady state regime, and this is similarly observed in the simulation results (Fig. 15). The pressure and temperature profiles are correlated: both pressure (Fig. 15) and temperature (Fig. 16) profiles decrease after second 1100 s

Fig. 15 Simulation vs. experimental pressure downstream the inlet valve and at the outlet of bladder; At 1100 s the bladder deflates
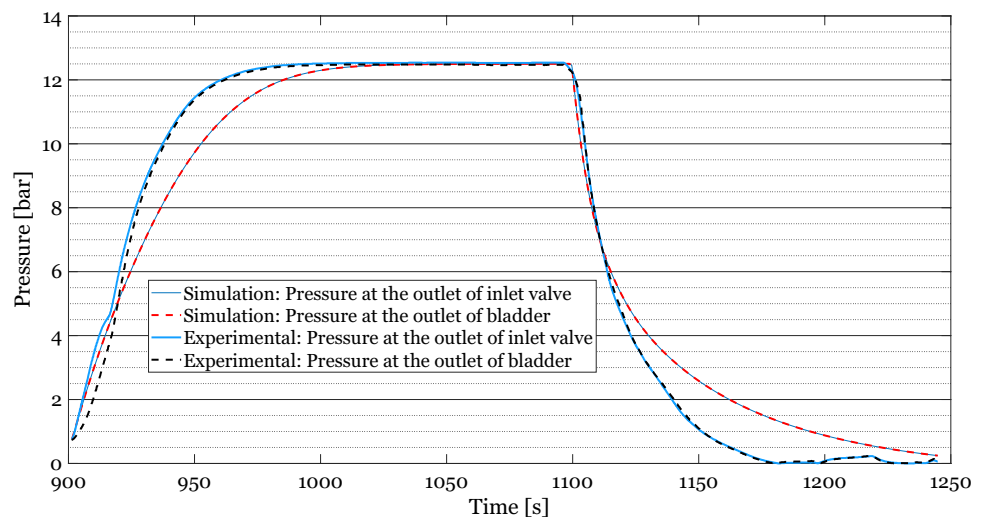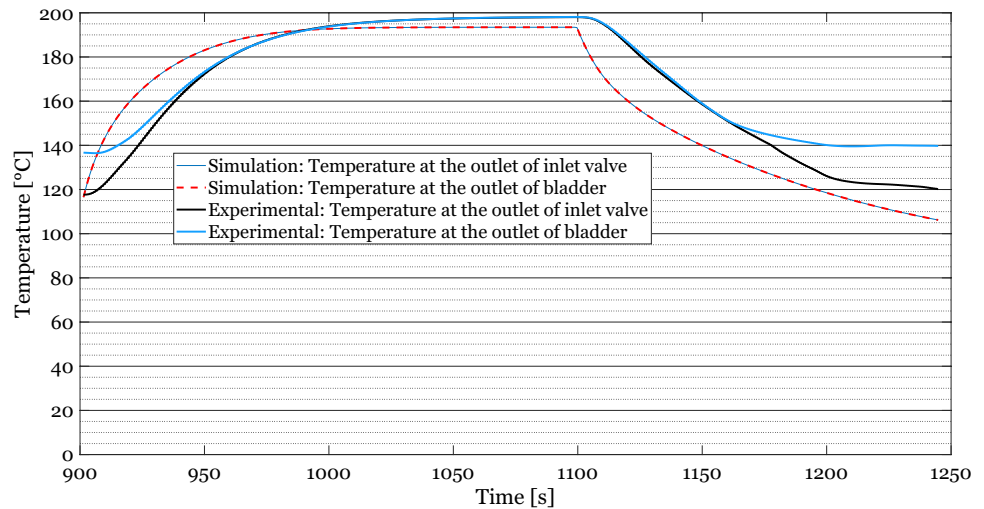
Fig. 16 Simulation vs. experimental temperature downstream the inlet valve and at the outlet of bladder

in the simulation. The numerical and experimental temperature profiles are also very similar. The temperature drop predicted by the simulation is faster than in the experimentally measured profile. This difference is due to the location of the sensor in the plant, which is placed right before the outlet valve.

Both valves are controlled by a time-controlled trigger, which allows the inlet valve to be opened at second 901.5 and remain open for 197.1 s until 1098.6 s; after this time the outlet valve is triggered to open until the end of the simulation at 1244.8 s. This behaviour is reflected by the mass flow rate profiles in Fig. 17.

4.4 Energy profiles

A very important outcome of the model is that the temporal profile of the energy received by the tyre can now be computed. The results are shown in Fig. 18: the energy stored in the tyre reaches 60 kJ with a maximum temperature of 186 °C, receiving energy from both the hot plates and the bladder. After about 1100 s, heat transfer from the bladder starts reducing, when the bladder begins contracting and eventually becomes negative since the bladder removes heat from the tyre instead of providing it. While the heat coming from the hot plates increases, this increment is not sufficient to compensate the cooling effect of the bladder, and the overall the energy stored by the tyre decreases from 60 down to about 54 kJ. This is an important result: the model says that the maximum energy is reached at about 975 s, and the remaining time is not significantly useful from an energetic point of view, i.e. it does not provide additional heat to the tyre. Of course, this does not mean that this time is wasted or useless, because the vulcanization reaction needs time to be deployed and because the final seconds at high gas pressure are required to calibrate the geometry. Nevertheless, Fig. 18 shows that some little reductions of process cycle time could be obtained with no losses of total energy transferred to the tyre, provided that this reduction does not

Fig. 17 Simulation vs. experimental mass flow rate at the outlet of inlet valve and at the outlet of outer valve
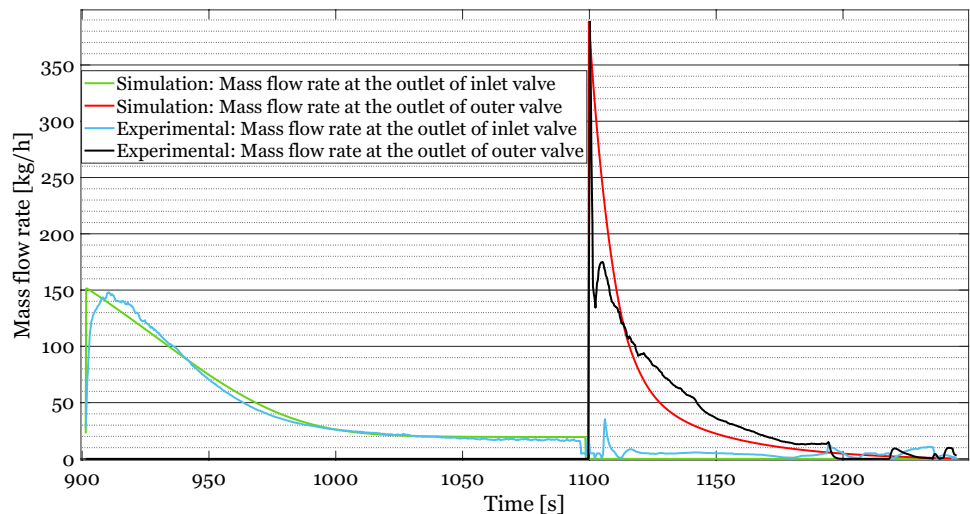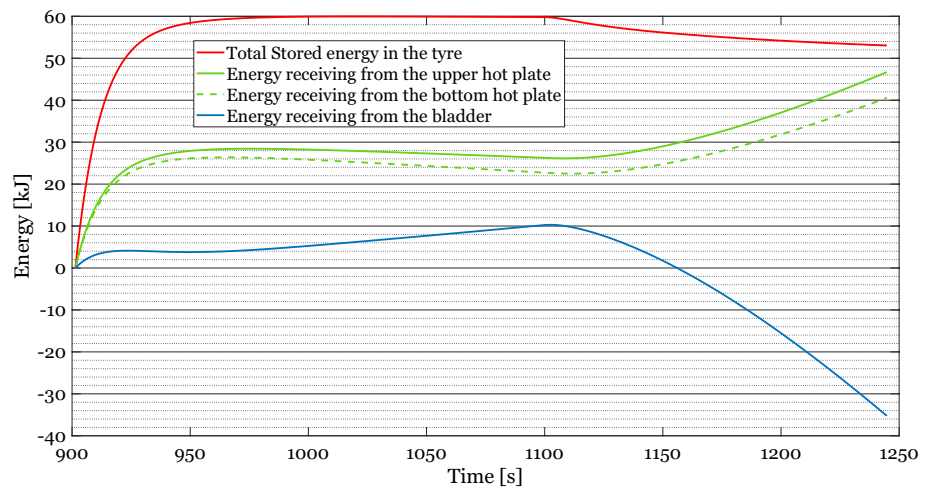
Fig. 18 Profiles of energy received by the tyre from the three heat sources

reduce the tyre quality. Non negligible energy savings can be obtained even with a small cycle time reduction, as later shown in Sect. 5.1.

5 Analysis of Energy Efficiency and discussion of results

The energy model, once validated experimentally, can now be used to compute some measures of energetic efficiency of the vulcanization process, both in the warm-up open press phase and in the curing phase.

During the warm-up phase, no tyre is present in the system, hence the efficiency EFR_{vulca} defined in Eq. (2) cannot be estimated. However, we can calculate how much energy is stored as heat by the system with respect to the total energy given. The fluid that exits the bottom hot plate is still hot, but its associated energy can be recovered by the centralised heating system only in a very small fraction, which is estimated to be not more than 10%. The results are summarised in Table 5. A very large amount of energy is spent to warm up the tooling (about 46,000 kJ), but the efficiency is relatively good, only 44% of this energy is wasted. Besides, this efficiency can be easily and rather inexpensively improved, by improving the insulation conditions of the metal masses to limit the radiation and convection exchange towards the environment. Furthermore, the warm-up phase is not very

critical, since it is a condition that happens only occasionally during the life span of the equipment.

Although the overall contribution of the warm-up phase is not relevant in the long run, Table 5 is useful because it shows that 32% of the total incoming energy is lost at the exit of the steam flow. It is very clear that heating by steam is unavoidably inefficient because the flow must keep enough enthalpy throughout the whole pipeline, otherwise it would not be able to transfer heat to the mould. Quite obviously, an alternative electric heating technique, either by electric resistance cartridges [45] or by induction coils [46], would reduce this source of losses almost to zero. Unfortunately, the rubber curing industry has been relying for many decades on the centralised production of steam through burning of fossil fuels, because this was the most economic way of doing it, regardless of its environmental impact and energetic efficiency. This means that there are many large factories with hundreds of vulcanization presses which are still, today, warmed-up by steam. An electric conversion would most likely, today, be strategically and economically convenient, but this conversion requires important capital investments that still represent the main limiting factor.

After the initial warm-up phase, the regular vulcanization cycle represents almost the totality of the operating time and therefore its environmental impact is crucial. In Fig. 19 and Table 6 the energy contributions and some efficiency measures are reported. The energy balance is such that the

Table 5 Energy efficiency of the equipment, during the warm-up phase

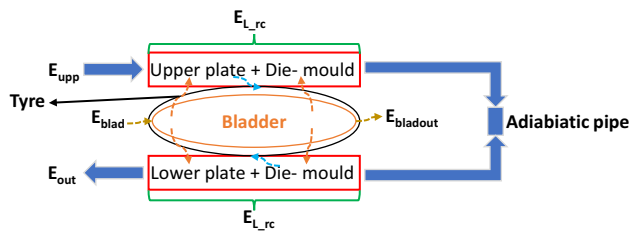|	
Direct Energy DE	Energy received by the upper hot plate (direct energy): $E_{upp} = DE = 46,120$ kJ (sensor 10)
Losses	Energy lost by convection and radiation: $E_{l\_rc} = 6095.6$ kJ (15 and 16 and similar)
	Energy outgoing the lower hot plate (90% of it is lost): $E_{out} = 16,564$ kJ (before 17 and 18)
Efficiency	Warm-up equipment Efficiency $EFR_{equip} = 100 \dfrac{E_{upp} - E_{l_{rc}} - 0,9E_{out}}{E_{upp}} = 56\%$

Fig. 19 Energy contributions during the curing phase

direct energy DE (6.7 MJ) is the sum of various contributions, listed and defined in Table 6:

$$DE = E_{upp} + E_{blad} + SE = E_{L\_RC} + E_{out} + E_{blad\_out} + VE \tag{3}$$

The value of EFR_{vulca} is only about 1%, an astonishingly low number, which is the consequence of the heating technology by steam, which is so inherently inefficient. Furthermore, we must consider that the quantities in Table 6 are computed only during the curing closed-press phase, which lasts about 350 s. After that, the press is opened, and the tyre is changed. While the press is open (for about 150 s), steam continues to circulate in the hot plates and the bladder is pre-heated and partly inflated before the insertion of a new tyre. In other words, the system energy SE which is consumed during curing is provided during the open press phase, with a presumed overall efficiency similar to the 56% calculated previously for the warm-up phase. If we had to compute EFR_{vulca} considering not only the curing phase, but the entire cycle, its value would further decrease to a value lower than 0,75%.

From a purely theoretical point of view, considering a heat capacity of about 2 kJ/(kg°C), the heat required to bring a 250 g tyre up to 175 °C starting from room temperature is about 75 kJ. The Amesim model estimates an energy absorption by the tyre of 60 kJ, which is well in the same order of magnitude (neglecting the heat generated by the exothermal reaction). This very lightweight bicycle tyre requires a tooling that consumes thousands of kJ, only to use a few tens. It is very clear, after reviewing the results of the energetic model, that heating hundreds of kg of steel, to warm a small tyre, must inevitably be a very inefficient operation. However, tremendous margins of improvements are available: by looking at Fig. 18, we can observe that the hot plates transfer a total of about 90 kJ during one cycle, while they consume thousands of kJ. Their efficiency could easily be improved, as stated above, by improving their outer insulation. On the contrary, the efficiency of the bladder is even negative, because it receives less than 4000 kJ, it first transfers only about 10 kJ to the tyre, but then it subtracts heat, for a total final balance of about -40 kJ. In other words, filling the bladder requires a considerable amount of enthalpy, because of its large inflated volume, but the thermal conditions are such that a very little amount of this energy is actually exchanged with the tyre. It is required to keep the internal surface of the bladder at a given temperature and pressure, but the same goal might be obtained with a more modern and more energy efficient technology. As an example, Zhang et al. [47] claim that a mechanical internal pressurization, electrically heated, system would allow to save up to of 86% of energy per curing cycle.

It is interesting to observe that while EFR_{equip} is above 50% in the warm-up phase, it is one order of magnitude smaller during the curing, closed-press, phase. This is entirely due to the additional energy brought by the bladder, which is practically entirely lost at the end of the curing phase. This means that while the steam heating technology can still be considered acceptable for the hot plates, it is dramatically inefficient for the bladder, and efficient alternatives need to be found and implemented soon.

The same Amesim model described in this paper has been modified and extended to predict the energy flows and efficiency of the curing process of a different case, the vulcanization of a car tyre with 457.2 mm outer diameter,

Table 6 Energy contributions and efficiency calculation during the curing phase in one cycle

Direct Energy DE	Energy entering the upper hot plate during the curing cycle: E_{upp} = 1822 kJ
	Energy entering the bladder during the curing cycle: E_{blad} = 3924 kJ
	Reduction of thermal energy stored in the system (tools + bladder) while curing SE: 950 kJ
Losses	Energy lost by convection and radiation: E_{L_RC} = 826 kJ
	Energy outgoing the lower hot plate (only 10% of it can be recovered): E_{out} = 1778 kJ
	Energy lost through the bladder discharge valve = E_{blad_out} = 4040 kJ
Vulcanization energy VE	Energy stored in the tyre: VE = 52 kJ
Efficiency	Efficiency of the curing cycle $EFR_{vulca} = 100 \frac{VE}{DE - 0,1E_{out}} = 0,8\%$
	Efficiency of the equipment $EFR_{equip} = 100 \frac{DE - E_{L\_RC} - 0,9E_{out} - E_{blad\_out}}{DE} = 3,4\%$

Fig. 20 Tooling setup for the curing process of a car tyre
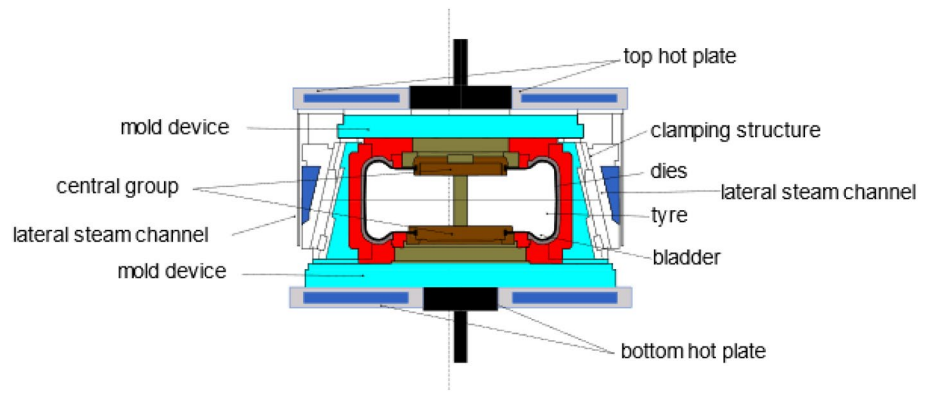
weighing 11.4 kg, about 57 times heavier than the bicycle tyre studied in the present paper. The tooling is more complex, with side inserts in addition to the upper and lower plates (Fig. 20). Two different gases are used in the bladder: steam at relatively low pressure to provide internal heating, nitrogen at high pressure to provide compression against the mould. The upper and lower plates and the side inserts in this case require a total input of 19 kg/h of steam. The numerical models proved to be very accurate also in this second test case. In this second case the value of DE is 32 MJ (about 5 times higher than the DE required for the bicycle tyre). VE is instead 2,9 MJ, more than 50 times higher than before. Since the VE value increases more than the DE value, the efficiency EFR_{vulca} is much better in this case, amounting to about 9,5%. Nevertheless, even for this heavier car tyre, more than 90% of the consumed energy is not actually spent by the curing process, but it is spent to let the machine operate.

The results here presented have been computed using the simulated values, although very similar efficiency indications can be obtained directly using the experimental measurements. However, the well validated simulation model can now be used for running sensitivity analysis, which cannot be easily obtained with the real press. In the next sub-section, the Amesim model is therefore used to evaluate the potential efficiency improvement that could be obtained with modifications of the systems and the process.

5.1 Sensitivity analysis, potential efficiency improvements

The simulation model allows to identify what possible changes on the process and on the equipment may be implemented to improve the energy efficiency and what energy savings can be predicted for each case.

The sensitivity has been run by assuming the following 4 cases, in addition to the base line, represented by the current situation described above.

(Case 1) The moulds are made of metal. Their external surfaces could be easily modified and covered with an insulating material, so that the environmental losses in the curing phase may be reduced by 50%.

(Case 2) Fig. 18 clearly show that the energy received by the tyre reaches its maximum in a time which is a small fraction of the total curing time. The curing time, though, must be long enough because the reticulation process is a relatively slow process and, therefore, the tyre needs to stay at a given temperature (and internal pressure) for some time in order to be fully cured. Nevertheless, hardly the total curing time is optimized with respect to quality and process engineers believe that there is some room for reducing the total time, improving productivity (and energy efficiency) without no significant loss of vulcanization quality. An assumption has been made that the process could be significantly reduced from 350 down to 270 s.

(Case 3) The improvements brought by cases 1 and 2 can be combined, to understand their joint effect.

Table 7 Energy savings that may derive from modification of the process of cases from 1) to 4) described above

	case	energies (kJ)								efficiency		
		E_{upp}	E_{blad}	SE	DE	E_{L_RC}	E_{out}	E_{blad_out}	VE	energy saved per cycle	EFR_{vulca}	EFR_{equip}
base	current conditions	1822	3924	950	6696	826	1778	4040	52	-	0,80%	3,43%
1	improved insulation of mould towards environment	1822	3924	538	6284	413	1777	4041	53	6%	0,87%	3,67%
2	reduced curing time to 4,5 min	1440	3590	799	5829	651	1397	3728	53	13%	0,93%	3,31%
3	improved insulation and reduced time	1440	3590	469	5500	326	1395	3726	53	18%	0,99%	3,50%
4	reduced curing time and increased pressure	1440	4606	728	6774	651	1397	4673	53	-1%	0,80%	2,84%

(Case 4) The current value of pressure inside the bladder is a little more than 12 bar. In case that the total time is reduced, the pressure might be simultaneously increased (up to 15 bar) in order to reduce the risk of a loss of the tyre quality.

The results of these four sensitivity study cases have been summarised in Table 7 and can now be commented. Improving the insulation of the moulds towards the environment (case 1) would allow to reduce the DE (direct energy employed in the process) from about 6,7 MJ down to about 6,3 MJ, with a 6% improvement.

If it was possible to reduce the curing time down to 4,5 min (case 2), without significant loss of quality, this would allow to save 867 kJ per curing cycle, with an energy saving of 13%.

If combining both the improved insulation and the reduced time (case 3), the energy saved would be 18%. Unfortunately, if reducing the curing time while simultaneously increasing the pressure (case 4) there would be no energy saving with respect to the base case. In all cases, the energy efficiency does not significantly change but, given the very large amount of energy that the process spends, significant improvements can be obtained even with the traditional heating technology by steam.

6 Conclusions

There is a general belief, among rubber industry experts, that the conventional tyre vulcanization process is dramatically inefficient. The model developed in the present work, and the direct measurements taken at the press, confirms this belief and demonstrates that the tyre industry urgently needs to convert to electrified heating methods.

The ratio between the net vulcanization energy VE and the direct energy DE spent to perform the process is extremely low, less than 1% for a 250 g bike tyre. This efficiency (EFR_{vulca}) increases to nearly 10% in case of a larger (about 11 kg) car tyre. In any case, the present work has shown that the conventional method of heating and inflating the bladder by means of water steam is a major source of inefficiency. While the steam heating technology can still be considered acceptable for the hot plates, the bladder is especially inefficient, because the heat transferred to the tyre is negligible in a first phase and it even becomes negative when the bladder is deflated. Dramatic energy efficiency improvements can therefore be achieved by improving the insultation conditions of the moulds and especially by searching for alternative and more efficient methods for heating and inflating the bladder.

The tyre industry is mostly based on rather conventional technologies, but these numbers clearly indicate that it is in strong need of a radical "green" conversion that may remove steam especially from the bladder, replacing it with a different heating medium.

Declarations

Conflict of interest On behalf of all authors, the corresponding author states that there is no conflict of interest.

Data transparency The simulations have been performed by the first author, who is available, upon request, at sharing the data.

References

1. Alkadi, F., Lee, J., Yeo, J.-S., Hwang, S.-H., & Choi, J.-W. (2019). 3D Printing of ground tire rubber composites. *International Journal of Precision Engineering and Manufacturing-Green Technology, 6*(2), 211–222. https://doi.org/10.1007/s40684-019-00023-6

2. Tan, Y., Dai, J., Wu, X., Wu, S., & Zhang, J. (2022). Characteristics, occurrence and fate of non-point source microplastic pollution in aquatic environments. *Journal of Cleaner Production, 341*, 130766. https://doi.org/10.1016/j.jclepro.2022.130766

3. Tian, X., et al. (2021). A novel approach of reapplication of carbon black recovered from waste tyre pyrolysis to rubber composites. *Journal of Cleaner Production., 280*, 124460. https://doi.org/10.1016/j.jclepro.2020.124460

4. n.a., "Project on Studying of Energy Efficiency Index in Rubber Industry," Bangkok, 2007. [Online]. Available: http://www2.dede.go.th/kmberc/datacenter/factory/rubber/RubberEng.pdf

5. Stankevičiūtė, L. (2000). *Energy Use and Energy Management in Tyre Manufacturing : the Trelleborg 1 Case*. Lund: Lund University.

6. Saidur, R., & Mekhilef, S. (2010). Energy use, energy savings and emission analysis in the Malaysian rubber producing industries. *Applied Energy, 87*(8), 2746–2758. https://doi.org/10.1016/j.apenergy.2009.12.018

7. Tsai, W.-H. (2018). Carbon taxes and carbon right costs analysis for the tire industry. *Energies, 11*(8), 2121. https://doi.org/10.3390/en11082121

8. Gudadhe, M., Lohakare, P., Meshram, M., & Padole, A. (2015). Energy analysis in tire manufacturing Industries. *International Journal of Mechanical Engineering Technology, 6*(9), 112–119.

9. Krishnan, A., Francis, R. M., Rahul Raj, K. R., Thomas, N., Muhammed Sadique, V. K., & Sriram, A. (2020). *Energy audit: a case study of tyre retreading unit in Kerala* (pp. 251–261). Springer Singapore.

10. Chikri YA, Wetzels W, (2019) Decarbonisation Options for the Dutch Tyre Industry. The Hague. [Online]. Available: www.pbl.nl/en

11. Sreelakshmi, M., Devika, J., John, A. T., & Deepa, O. S. (2021). Reducing the time delay in curing process by the implementation of DMAIC in tyre production. *Advances in industrial and production engineering* (pp. 465–478). Springer Singapore. https://doi.org/10.1007/978-981-33-4320-7_42

12. Shanbag, A., & Manjare, S. (2020). Life cycle assessment of tyre manufacturing process. *Journal of Sustainable Development of Energy, Water and Environment Systems, 8*(1), 22–34. https://doi.org/10.13044/j.sdewes.d7.0260

13. Lechtenböhmer, S., Nilsson, L. J., Åhman, M., & Schneider, C. (2016). Decarbonising the energy intensive basic materials industry through electrification – Implications for future EU electricity demand. *Energy, 115*, 1623–1631. https://doi.org/10.1016/j.energy.2016.07.110

14. Guo, J., Li, H., Yang, H., & Zhang, S. (2018). A collaborative detection approach for internal steam leakage of tyre vulcanization workshop with artificial immune algorithm. *Computational and Applied Mathematics, 37*(4), 4219–4236. https://doi.org/10.1007/s40314-017-0569-z

15. Tharmapalan E, Sivalingam S, Seyyaf NM, Kanagalingam N, Balasooriya LC, Nissanka ID, (2020) Performance Improvement of Industrial Induction Mould Heating Oven. In Moratuwa Engineering Research Conference (MERCon), pp. 602–607

16. Zhang, J., Tan, J., Liu, X., & Yang, W. (2016). Energy saving curing and precision manufacturing technology of tires. *In AIP Conference Proceedings, 130002*, 130002. https://doi.org/10.1063/1.4942334

17. You, J.-H., Lee, J.-W., Oh, S.-H., & Park, K. (2022). Conformal mold heating and cooling using a carbon nanotube film heater and additively manufactured cellular metamaterial. *International Journal of Precision Engineering and Manufacturing Technology, 9*(6), 1463–1476. https://doi.org/10.1007/s40684-021-00407-7

18. Kim, J., Mun, S. C., Ko, H.-U., Kim, K.-B., Khondoker, M. A. H., & Zhai, L. (2012). Review of microwave assisted manufacturing technologies. *International Journal of Precision Engineering and Manufacturing, 13*(12), 2263–2272. https://doi.org/10.1007/s12541-012-0301-2

19. Chang, P.-C., & Hwang, S.-J. (2006). Experimental investigation of infrared rapid surface heating for injection molding. *Journal of Applied Polymer Science, 102*(4), 3704–3713. https://doi.org/10.1002/app.24515

20. Yan, X., & Tong, J. (2003). Finite element analysis of tire curing process. *Journal of Reinforced Plastics and Composites, 22*(11), 983–1002. https://doi.org/10.1177/073168403026768

21. Han, I., et al. (1996). Dynamic simulation of the tire curing process. *Tire Science Technology, 24*(1), 50–76. https://doi.org/10.2346/1.2137512

22. Lopes, H., Silva, S. P., Carvalho, J. P., & Machado, J. (2022). A new modelling approach for predicting process evolution of cork-rubber composites slabs vulcanization. *Science and Reports, 12*(1), 8002. https://doi.org/10.1038/s41598-022-11849-7

23. Han, I. S., Chung, C. B., Jeong, H. G., Kang, S. J., Kim, S. J., & Jung, H. C. (1999). Optimal cure steps for product quality in a tire curing process. *Journal of Applied Polymer Science, 74*(8), 2063–2071. https://doi.org/10.1002/(SICI)1097-4628(19991121)74:8%3c2063::AID-APP22%3e3.0.CO;2-V

24. Yang, H.-D., Liu, G.-S., Huang, G. Q., & Chen, X. (2013). Statistical modeling for energy consumption and anomaly detection in rubber vulcanization process. *Journal of Energy Engineering, 139*(2), 65–71. https://doi.org/10.1061/(asce)ey.1943-7897.0000098

25. Guilong, W., Guoqun, Z., Huiping, L., & Yanjin, G. (2010). Analysis of thermal cycling efficiency and optimal design of heating/cooling systems for rapid heat cycle injection molding process. *Materials and Design, 31*(7), 3426–3441. https://doi.org/10.1016/j.matdes.2010.01.042

26. Guo, J., & Yang, H. (2015). A fault detection method for heat loss in a tyre vulcanization workshop using a dynamic energy consumption model and predictive baselines. *Applied Thermal Engineering, 90*, 711–721. https://doi.org/10.1016/j.applthermaleng.2015.07.064

27. Schmidt, C., Li, W., Thiede, S., Kara, S., & Herrmann, C. (2015). A methodology for customized prediction of energy consumption in manufacturing industries. *International Journal of Precision Engineering and Manufacturing-Green Technology, 2*(2), 163–172. https://doi.org/10.1007/s40684-015-0021-z

28. Milani, G., & Milani, F. (2021). Relation between activation energy and induction in rubber sulfur vulcanization: an experimental study. *Journal of Applied Polymer Science, 138*(12), 50073. https://doi.org/10.1002/app.50073

29. Fekiri N, Canto C, Madec Y, Mousseau P, Plot C, Sarda A, (2017) Design and thermal analysis of a mold used in the injection of elastomers. In Esaform p. 120009 https://doi.org/10.1063/1.5008147

30. Garcìa Jarabo, A. (2018). *Energetic modelling and efficiency improvement of a tyre vulcanization press*. Politecnico di Milano.

31. Adam, Q., Behnke, R., & Kaliske, M. (2020). A thermo-mechanical finite element material model for the rubber forming and vulcanization process: From unvulcanized to vulcanized rubber. *International Journal of Solids and Structures, 185–186*, 365–379. https://doi.org/10.1016/j.ijsolstr.2019.08.037

32. Mark, J. E., Erman, B., & Roland, M. (Eds.). (2013). *The science and technology of rubber* (4th ed.). Academic Press.

33. Alcalá, N., Castrillón, M., Viejo, I., Izquierdo, S., & Gracia, L. A. (2022). Rubber material-model characterization for coupled thermo-mechanical vulcanization foaming processes. *Polymers (Basel), 14*(6), 1101. https://doi.org/10.3390/polym14061101

34. Princi, E. (2019). *Rubber: Science and technology*. De Gruyter.

35. Mucci, S., Bischi, A., Briola, S., & Baccioli, A. (2021). Small-scale adiabatic compressed air energy storage: Control strategy analysis via dynamic modelling. *Energy Conversion and Management., 243*, 114358. https://doi.org/10.1016/j.enconman.2021.114358

36. Deshmukh, A., & Kapat, J. (2020). Pinch point analysis of air cooler in supercritical carbon dioxide brayton cycle operating over ambient temperature range. *Journal of Energy Resources Technology.* https://doi.org/10.1115/1.4046083

37. Maghrabie, H. M., et al. (2022). Numerical simulation of heat pipes in different applications. *International Journal of Thermofluids, 16*, 100199. https://doi.org/10.1016/j.ijft.2022.100199

38. Zhou, C., Yu, N., Wang, J., Jin, P., & Cai, G. (2021). Analysis of dynamic characteristics and sensitivity of hydrogen-oxygen expansion cycle rocket engine system. *Acta Astronautica, 189*, 624–637. https://doi.org/10.1016/j.actaastro.2021.08.046

39. Liu, M., Wu, D., Tsolakis, A., & Gao, W. (2021). A waste cryogenic energy assisted freshwater generator for marine applications. *Desalination, 500*, 114898. https://doi.org/10.1016/j.desal.2020.114898

40. Zhou, X., Chen, H., Liang, K., Wang, W., Dong, B., & Zhang, Y. (2022). Winter performance analysis of multi-mode integrated thermal management system based on thermodynamics. *Sustain. Energy Technology Assessments, 53*, 102726. https://doi.org/10.1016/j.seta.2022.102726

41. Wei, D., Cui, Z., & Chen, J. (2008). Optimization and tolerance prediction of sheet metal forming process using response surface model. *Computational Materials Science, 42*(2), 228–233.

42. Zhao, D., Ge, W., Mo, X., Liu, B., & Dong, D. (2019). Design of a new hydraulic accumulator for transient large flow compensation. *Energies, 12*(16), 3104. https://doi.org/10.3390/en12163104

43. Zhang, Z., Guo, F., Ke, Y., Xiang, C., & Jia, X. (2022). Effect of vulcanization on deformation behavior of rubber seals: thermal–mechanical–chemical coupling model, numerical studies, and experimental validation. *Material and Design, 224*, 111314. https://doi.org/10.1016/j.matdes.2022.111314

44. Xu, Y., Fang, X., Su, X., Zhou, Z., & Chen, W. (2012). Evaluation of frictional pressure drop correlations for two-phase flow in pipes. *Nuclear Engineering and Design, 253*, 86–97. https://doi.org/10.1016/j.nucengdes.2012.08.007

45. Bosselmann, S., Frank, T., Wielitzka, M., & Ortmaier, T. (2018). Optimization of process parameters for rubber curing in relation to vulcanization requirements and energy consumption. *IEEE/ASME International Conference on Advanced Intelligent Mechatronics (AIM)*. https://doi.org/10.1109/AIM.2018.8452354

46. Karpushkin, S. V., Karpov, S. V., & Glebov, A. O. (2011). Modeling of induction heating devices in example of induction heating platens of vulcanization presses. *Transactions TSTU, 17*(1), 110–120.

47. Zhang, J., et al. (2020). Energy-saving performance and production accuracy of the direct-pressure tire curing technology with an expandable steel internal mold. *Applied Sciences, 10*, 79. https://doi.org/10.3390/app10010079

Publisher's Note Springer Nature remains neutral with regard to jurisdictional claims in published maps and institutional affiliations.

Paolo Albertelli has been developing his research activities as an Assistant Professor of the Mechanical Engineering Department (academic discipline ING-IND/16) of Politecnico di Milano since December 2011. His research has been focused mainly on the development of Advanced Manufacturing Solutions and Manufacturing Processes Sustainability. More specifically, a branch of his research deals with Machine Tool dynamics and cutting stability. Regenerative chatter modelling, cutting stability prediction, chatter monitoring, vibration suppression and the development of advanced monitoring solutions are some of the covered topics. He is also working on Prognostics and Health Management PHM of Machine Tools and their functional modules. Another branch of his research is focused on Energy consumption (assessment, identification, modelling and reduction) in Machine Tools, in linked subunits and in other Automatic Machines. Moreover, he is working on cryogenics as a feasible and sustainable solution for machining hard to cut materials and for some forming processes. He is the author of more than 40 publications in peer-reviewed journals and international conferences. He permanently collaborates with companies and specifically with machine tools manufacturers.

Matteo Strano is associate professor of Manufacturing Systems and Technologies at the Dipartimento di Meccanica of Politecnico di Milano, in the research group of Sustainable Smart Manufacturing. He is the author of 135 publications of different type starting from year 2001, including scientific papers in peer revied journals, presentations at conferences, chapters in books, educational books and technical articles in specialised magazines. He teaches Advanced Manufacturing Processes. He is an active member of AITEM (the Italian Association of mechanical Manufacturing Systems and Technologies) and of ESAFORM (the European association for materials forming). In the last few years, his research activities have been focused on additive manufacturing of rapid tools by extrusion and on methods for improving the sustainability of materials forming processes, such as energy savings approaches, advanced FEM based optimization of processes, techniques for reducing the use of lubricants in manufacturing processes.

Lohit Kumar Pentakota is a mechanical engineer, he took his bachelor degree in Amity University of Mumbai in 2018 and his master title at Politecnico di Milano in 2021, with a thesis on the thermal modelling of a vulcanization press. He then worked as a research fellow at the lab MUSP (Macchine Utensili e Sistemi di lavorazione) in Piacenza, dealing with several R&D projects, including the simulation of manufacturing equipment. He is currently working at the CNR-STIIMA research institute in Milan.